scientific reports

Check for updates

OPEN

Robotic radiation shielding system reduces radiation-induced DNA damage in operators performing electrophysiological procedures

Ziv Sevilya[1,4]✉, Michael Rahkovich[1], Yonatan Kogan[1], Gergana Marincheva[1], Michal Cipok[2], Vera Hershkovitz[2], Erez Barenboim[3,4], Eli Israel Lev[1,3] & Avishag Laish-Farkash[1,3]

Fluoroscopically guided electrophysiology (EP) procedures expose operators to low doses of ionizing radiation, which can induce DNA double-strand breaks (DSBs) and raises increasing concerns regarding potential health risks. A novel robotic radiation shielding system (RSS) was developed to provide full-body protection by encapsulating the imaging beam and blocking scattered radiation. This study aimed to compare the levels of blood lymphocytes expressing DSB markers, pATM and γ-H2AX, in operators performing EP-procedures with and without RSS. Radiation dose exposure was significantly higher without RSS ($p = 0.0278$). The level of cells expressing pATM and γ-H2AX was linear correlated with radiation exposure, with neither marker detected at doses below 13.4 µSv. Without RSS, the level of pATM or γ-H2AX positive cells increased significantly immediately after the procedure (8.6-fold, $p < 0.0001$ and 3.4-fold, $p = 0.0279$, respectively). After 4 h, marker levels were moderately reduced, and at 24 h, pATM returned to baseline and γ-H2AX decreased to 1.9-fold over baseline ($p = 0.9739$). In contrast, with RSS, no significant elevation in pATM or γ-H2AX positive cells was observed, suggesting no significant DSB formation. In conclusion, the use of an effective full-body protection system during fluoroscopically guided EP-procedures may help mitigate DSB formation and reduce the genotoxic health risks for operators.

Keywords X-ray radiation, Radiation protection, DNA repair, Double strand breaks, Ablations, CIED

Fluoroscopically guided electrophysiologic (EP) interventions, including ablations and the implantation of cardiac implantable electronic devices (CIED), expose operators to repeated low-level ionizing radiation (IR), which poses a significant health risk[1]. Studies suggest an association between fluoroscopically-guided EP interventions and an increased risk of adverse health effects, such as cataracts and malignancies[1-7]. Additionally, studies suggest potential association between long-term exposure of radiologists to low-dose IR and dysfunction of the central nervous system, circulatory disease, cardiovascular disease, solid tumors and leukemia associated in[8-9].

The low-dose range of IR is defined as cumulative radiation below 100 mGy, according to the classification proposed by the United Nations Scientific Committee on the Effects of Atomic Radiation[11]. Risk assessment due to exposure to low-level IR is currently evaluated by extrapolation from the risks observed at high acute dose exposures, such as data from atomic bomb survivors in Hiroshima and Nagasaki, and follow-up studies after nuclear accidents, according to the Linear No Threshold (LNT) hypothesis[10,12]. The LNT hypothesis assumes that the cancer risk is directly proportional to the dose received, with no threshold, and forms the basis of the radiological protection system. Other models suggest a possible existence of a dose threshold, while some suggest that the relationships between the dose received and the risk effect is supra-linear, indicating that the LNT model underestimate the risk in low doses of IR[13].

IR induces DNA damage, which includes oxidative DNA/base damages, apurinic/apyrimidinic (AP) sites, DNA single-strand breaks, and most notably, double-strand breaks (DSB). DSBs can result in the loss of large chromosomal regions and require rapid repair. In dividing mammalian cells, there are an estimated ten DNA DSBs per day per cell, arising from IR, reactive oxygen species, and DNA replication errors[14]. DSB can produce mutations, loss of heterozygosity, and chromosome rearrangements that can result in cell death or cancer[15,16].

[1]Cardiology Department, Assuta Ashdod Medical Center, Ashdod, Israel. [2]Hematology Laboratory, Assuta Ashdod Medical Center, Ashdod, Israel. [3]Ben-Gurion University of the Negev, Beer-Sheva, Israel. [4]Assuta Ashdod Medical Center, Harefua 7, Ashdod, Israel. ✉email: zivse@assuta.co.il

DSBs induce an immediate response from the Mre11-Rad-50 Nbs1 complex, which causes rapid phosphorylation of Ataxia Telangiectasia Mutated (ATM) protein[17]. The phosphorylated ATM (pATM) protein leads to phosphorylation of downstream targets involved in cell cycle checkpoints and DNA repair signal transduction processes. ATM induces phosphorylation of Histone H2AX at Serine 139 residue (γH2AX)[14]. The γH2AX protein serves as a docking site for DNA damage and repair proteins to promote DSB repair[18]. Expression of pATM and γH2AX proteins in circulating lymphocytes is a sensitive biomarker of radiation-induced DSBs and acute response of DNA damage response and repair mechanisms[19,20]. Measuring the level of circulating lymphocytes expressing the pATM and γ-H2AX biomarkers can serves as an indicator of the biological response to IR exposure.

Circulating lymphocytes are sensitive to radiation, and their biological response can serve as a surrogate biomarker for low-dose exposure to radiation[21-23]. El-Sayed et al. (2017) detected an acute DNA damage response in operators performing fluoroscopic-guided endovascular aortic repair procedures by quantifying the percentage of pATM and γH2AX proteins expression in peripheral blood mononuclear cells (PBMCs)[24]. Moreover, an increased incidence of chromosomal aberrations has been reported in operators performing a large volume of endovascular procedures[25]. To date, the DNA damage response in operators performing EP-procedures has not been investigated.

Current radiation protection for interventional personnel includes advanced imaging systems, personal protective clothing, ceiling-mounted shields, and table-skirts. Recently, we tested a novel robotic radiation shielding device, the Radiaction Shielding System (RSS), which provides full-body protection to all medical personnel during fluoroscopic-guided procedures by encapsulating the imaging beam and blocking scattered radiation[26,27]. In a prospective study for both CIED and ablation procedures, the radiation exposure with RSS was significantly lower than without RSS. For ablation procedures, there was an 87% (76–97% for the different sensors in various locations in the EP laboratory) reduction in radiation compared to standard radiation protection. For CIED implantations, there was an 83% reduction in radiation (59–92% for the different sensors)[27].

In the present study, we aimed to investigate the biological effects of the novel robotic radiation shielding system in fluoroscopically-guided EP interventions by measuring the percentage of pATM and γH2AX positive cells in circulating lymphocytes after the procedures with and without RSS. We also evaluated individual operators' responses to radiation and the kinetics of pATM and γH2AX proteins with and without RSS. Evidence from studies involving human populations exposed to IR is particularly valuable, as it eliminates the need to extrapolate findings from molecular, cellular, tissue, or animal models to humans.

Results

Induction of pATM and γH2AX in lymphocytes following EP procedures with or without RSS

Overall, twenty experiments were performed with four operators. Ten of them were conducted without RSS protection, and the other ten with RSS. The EP procedures are described in Table 1. The procedures type and specific projection angles were similar with and without RSS protection (Table 1). The median fluoroscopy time without RSS was 1410 (IQR 1120–1963) seconds and with RSS was 1711 (IQR 997–2344) seconds ($p = 0.6842$) (Fig. 1a).

Operator	Operation type	RSS	Procedure time, hr: min	Fluoroscopy Time, seconds	DAP, GyM^2	Sensor read, μSv	Most common angle.
A	PVI Cryo	-	1:00	1457	0.002374	54.8	LAO
A	SVT	-	2:24	2220	0.000025	90.2	AP/LAO
A	ICD + ICD	-	2:26	955	0.001010	51.5	AP
A	PVI Helius Carto	+	1:53	2176	0.008469	1.6	LAO
A	Redo PVI Carto	+	2:57	1763	0.009567	55.5	LAO
A	CRTD	+	2:30	1658	0.004051	13.4	AP/LAO
B	PVI Helius Carto	-	1:40	1363	0.002433	16.6	LAO
B	Ablation VT Carto	-	1:37	2010	0.006563	29.3	AP/LAO
B	PVI Helius Carto	-	2:15	1822	0.005915	50.5	LAO
B	ICD	+	0:49	217	0.000673	6.1	AP
B	PVI Cryo + CTI	+	2:05	2400	0.003015	1.7	LAO/LAO
B	PVI Cryo	+	2:31	3550	0.013515	15	LAO
C	PVI Cryo + ICD + PPM	-	2:28	1250	0.002983	35.2	LAO/AP/AP
C	PVI	-	1:32	512	0.001565	58.9	LAO
C	Cryo + EPS + PPM + PPM	-	3:38	2477	0.004254	185.1	LAO/AP/AP/AP
C	CRTD + PPM + PPM	+	4:23	780	0.000399	50.6	AP/LAO/AP
C	PVI Cryo + RT CRTD	+	3:43	4153	0.015694	12.6	LAO/AP/LAO
C	ICD + EPS	+	2:21	1649	0.003818	9.5	AP/AP
D	CRTD	-	1:25	2477	0.002347	126.8	AP/LAO
D	ICD	+	1:25	239	0.000211	26.1	AP

Table 1. Procedures characteristics.

The median Dose Area Product (DAP) for procedures without RSS was 0.0027 Gy/m^2 (IQR 0.0023–0.0055) compared to 0.0045 Gy/m^2 (IQR 0.0007–0.0096) for procedures with RSS ($p = 0.4561$) (Fig. 1b). The median reading from personal dosimeters placed over the operator's chest lead apron during procedures without RSS was significantly higher than with RSS [median 53.2 µSv (IQR 39.1–82.4) and 15.0 µSv (IQR 6.1–50.6), respectively] ($p = 0.0278$) (Fig. 1c). There was an 85% reduction (IQR 55 −89%) in the radiation normalized by DAP for operations with RSS compared to operations without RSS [median 37,693 µSv/(Gy/m^2 (IQR 7,252–87,750) and 5,801 µSv/(Gy/m^2 (IQR 803–39,059)), respectively], although the median DAP and irradiation time were comparable (Fig. 1d). No correlation was observed between the radiation dose measured in the operator's personal dosimeters and the DAP (Fig. 1e).

Flow cytometry analysis was performed on whole blood samples to quantify the levels of circulating CD3$^+$ lymphocytes expressing the DNA damage markers pATM and γ-H2AX before, immediately-after, 4 h after, and 24 h after EP procedures with or without RSS. The whole blood samples were lysed, fixed, permeabilized and incubated with antibodies against pATM and γH2AX proteins. The lymphocytes were gated according to the expression of CD3 receptor, and pATM and γH2AX positive CD3 cells were quantified (Fig. 2).

The level of positive cells for either pATM or γH2AX immediately post-procedure shows a linear correlation with the radiation exposure readings obtained from the personal dosimeters placed over the operator's chest lead apron ($R^2 = 0.6718$ ($p < 0.0001$) and $R^2 = 0.4808$ ($p < 0.0007$), respectively) (Fig. 3a and b). No correlation was observed between the level of pATM or γH2AX positive cells and the DAP measurements (Fig. 3c and d). Importantly, at radiation dose above 59µSv, a high response of both pATM and γH2AX were observed (4 samples). At doses below 13.4 µSv, there was no significant increase in the proportion of pATM- or γH2AX-

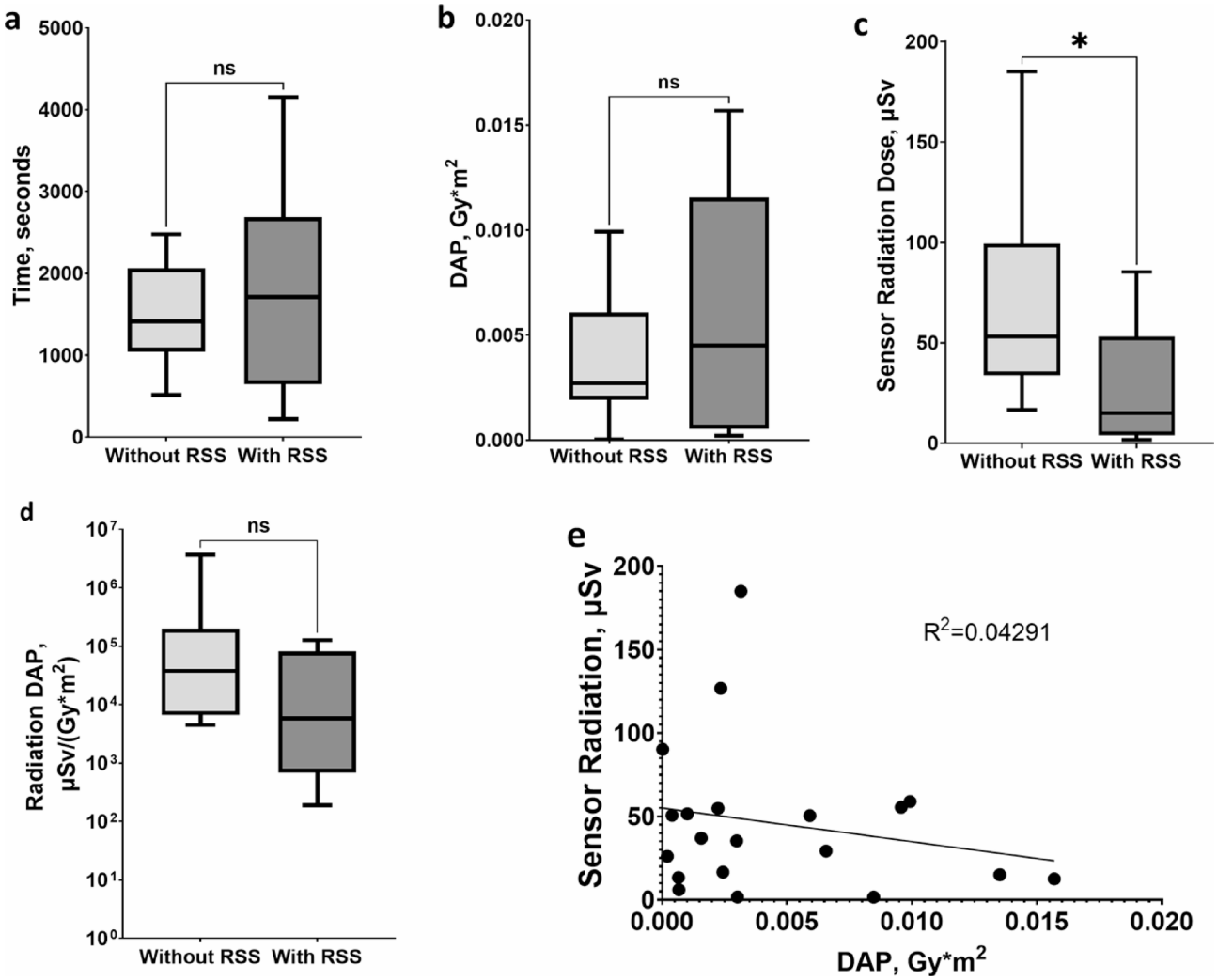

Fig. 1. Radiation exposure during electrophisiological procedures with or without RSS. **A**. Fluoroscopy time. **B**. Dose area product (DAP). **C**. Operators' chest sensor radiation dose. **D**. Radiation DAP. **E**. Correlation between operators' sensor radiation and DAP. Procedures were performed with (n=10) or without (n=10) RSS. Box and Whisker plot indicating the minimum, lower quartile, median, upper quartile and maximum. *p <0.05.

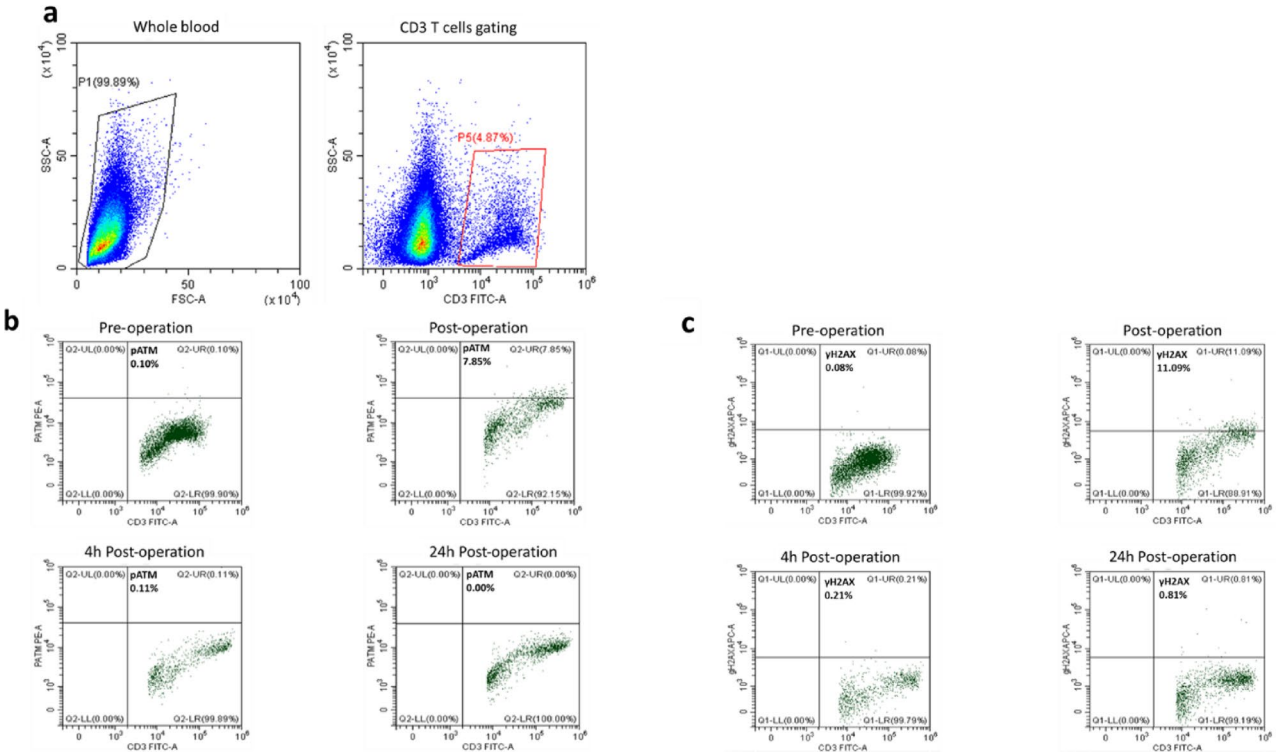

Fig. 2. Flow cytometry analysis of the percentage of pATM and γH2AX positive lymphocytes. Whole blood samples from operators were lysed, fixed, permeabilized, and stained with anti-CD3, pATM and γH2AX antibodies. **A**. Representative pseudo-color plot for lymphocyte gating according to forward and side scatter profile and expression of CD3. **(B)** Representative flow cytometric dot plots for pATM expression in $CD3^+$ cells obtained from the operator pre-procedure, immediately after procedure, 4 h post, and 24 h following EP procedure. **(C)** Representative flow cytometric dot plots for γH2AX expression in $CD3^+$ cells obtained from the operator pre-procedure, immediately after the EP procedure, 4 h post, and 24 h following the procedure.

positive cells relative to baseline levels (6 samples). Between 15 and 55.5μSv, 50% of the samples demonstrated level of cells positive for pATM and γH2AX above the baseline (5 out of 10 samples) (Fig. 3a and b).

Without RSS protection, the median percent of CD3 T cells expressing pATM increased from 0.8% (IQR 0.7–2.0) before the procedure to 6.9% (IQR 2.4–9.9) immediately after the procedure (8.6-fold increase, $p < 0.0001$, Fig. 4a; Table 2). CD3 T cells expressing γH2AX increased from 0.9% (IQR 0.6 −1.2) before the procedure to 3.1% (IQR 2.1–3.5) immediately after the procedure (3.4-fold increase, $p = 0.0279$, Fig. 4b; Table 2). Four hours after the procedures, 5.0% (IQR1.5-7.1) of CD3 T cells expressed pATM and 2.9% (IQR2.2–4.7) express γH2AX (6.3-fold increase, $p = 0.1735$, and 3.2-fold increase, $p = 0.046$, respectively). Twenty-four hours after the procedure, the fraction of pATM- expressing cells was reduced 4-fold from the measurement immediately post-procedure to 1.7% (IQR 0.8–2.7) ($p = 0.0003$), which is comparable to the baseline ($p = 0.9359$). The fraction of γH2AX-expressing cells was reduced by 1.8-fold from the measurement immediately post-procedure to 1.7% (IQR 0.7–2.3) ($p = 0.0551$), which is 1.9-fold above the baseline ($p = 0.9739$).

The median percent of CD3 T cells expressing pATM or γH2AX before the procedures with RSS protection (the RSS baseline) were 0.4% (IQR 0.2–0.5) and 0.5% (IQR 0.3–0.8), respectively (Fig. 4a and b; Table 2). Immediately after the procedures with RSS protection, the cell fraction expressing pATM or γH2AX were 0.2% (IQR 0.1–0.3) and 0.2% (IQR 0.1–0.2), respectively, which are comparable to the baseline pATM and γH2AX expression level ($p = 0.3822$ and 0.1092, respectively). The median expression of pATM and γH2AX 4 h after the procedure were 0.5% (IQR 0.2–1.8) and 0.3% (IQR 0.2–0.7), respectively. The fold change from the baseline for pATM 4 h after the procedures is 1.2 (IQR 0.9–4.2) with $p = 0.9860$, and for γH2AX the fold change is 0.6 (SQR 0.5–0.9) with $p = 0.5541$. The median percentage for pATM-expressing cells 24 h following the procedures was 0.4% (IQR 0.3–0.6), which is 1.1-fold (IQR 0.9–1.4) over the baseline ($p = 0.3150$). The median percentage for γH2AX-expressing cells 24 h following the procedures was 0.7% (IQR 0.4–0.9), which is 1.4-fold (IQR 1.1–1.2) over the baseline ($p = 0.9319$). The relatively high interquartile range observed is due to the low pATM and γH2AX expression. Overall, the expression levels of pATM and γH2AX were not significantly increased following the procedures performed with the presence of RSS protection.

As an assay positive control, we measured the percentage of pATM and γH2AX positive cells in blood samples obtained from operators immediately before each procedure and directly exposed to the radiation during the procedure. The median radiation dose for the positive control per procedure was 130.5 μSv (IQR 44.6-311.2). The positive control median fraction of pATM- expressing cells was 5.6% (IQR 2.1–6.3,) and for γH2AX, median fraction was 5.6% (IQR 3.0-9.2).

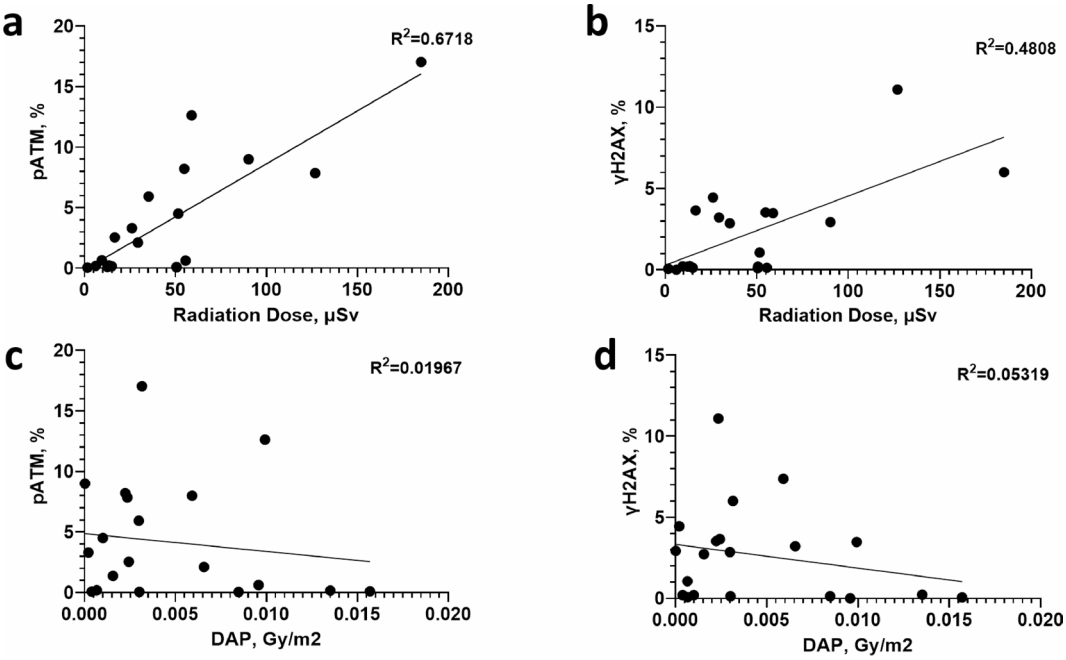

Fig. 3. Correlation between radiation dose and the percentage of pATM and γH2AX positive lymphocytes. Blood samples were obtained immediately post-procedure with or without RSS ($n = 20$) and the percentage of pATM or γH2AX positive cells was tested. **(A)** Percent of positive pATM cells as a function of the radiation dose. **(B)** Percent of positive γH2AX cells as a function of the radiation dose. **(C)** Percent of positive pATM cells as a function of DAP. **(D)** Percent of positive γH2AX cells as a function of DAP.

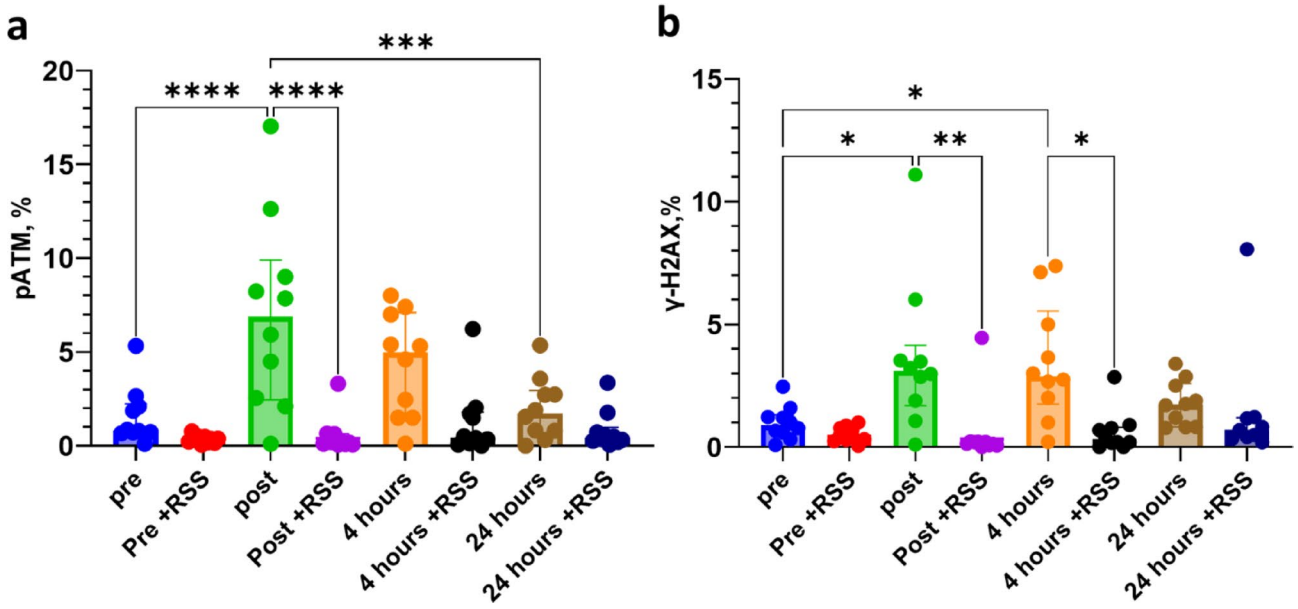

Fig. 4. Operators' percentage of pATM and γH2AX positive lymphocytes with or without RSS protection. Blood samples were collected before (pre), immediately-after (post), 4 h after, and 24 h after EP procedures. Three operators were re-tested on three separate days, and one operator was tested once ($n = 10$), with or without RSS, as indicated. The percent of pATM and γH2AX positive cells was measured using flow cytometry. **(A)** Percentage of pATM positive cells with or without RSS protection. **(B)** Percentage of γH2AX positive cells with or without RSS protection. Box limits (bold lines) indicate the medians, and the interquartile range is indicated by whisker extending from the bold lines. * $p \leq 0.05$, ** $p \leq 0.01$, *** $p \leq 0.001$, **** $p \leq 0.0001$, ns $p > 0.05$.

RSS	Marker	post		4 h		24 h	
		Fold change	*P* value	Fold change	*P* value	Fold change	*P* value
-	pATM	8.6	0.0001	6.3	0.1735	2.1	0.9359
-	γH2AX	3.4	0.0279	3.2	0.046	1.9	0.9739
+	pATM	0.5	0.3822	1.2	0.9860	1.1	0.3150
+	γH2AX	0.4	0.1092	0.6	0.5541	1.4	0.9319

Table 2. Fold change of percentage of pATM- and γH2AX-positive lymphocytes.

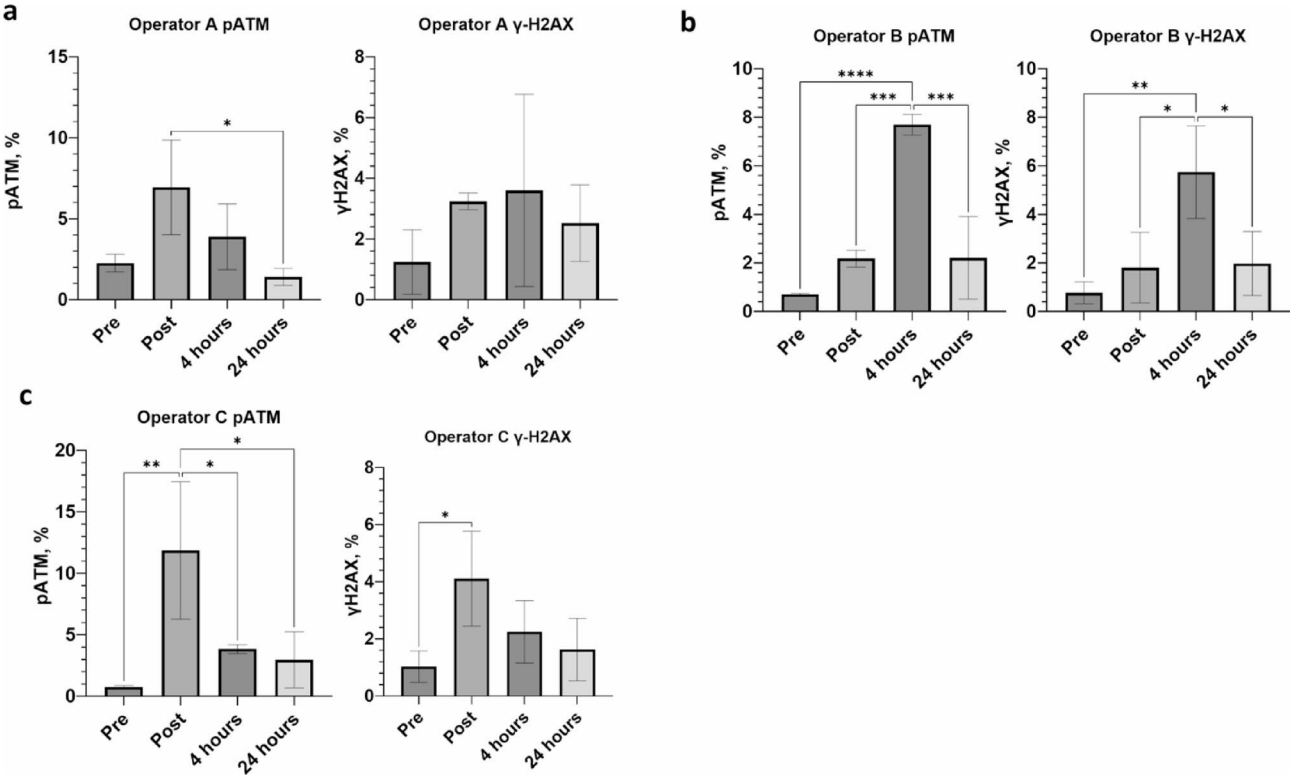

Fig. 5. Operators' percentage of pATM and γH2AX positive lymphocytes in each operator. The operators were re-tested on three separate days without RSS. **(A)** The mean fraction of pATM or γH2AX positive cells pre-, post-, 4 h, and 24-hours following procedures performed by operator A. **(B)** The mean fraction of pATM or γH2AX positive cells pre-, post-, 4 h, and 24 h following procedures performed by operator B. **(C)** The mean fraction of pATM or γH2AX positive cells pre-, post-, 4 h, and 24 h following procedures performed by operator C. The mean and standard deviation are indicated.

Variability of pATM and γH2AX expression among operators

Figure 5 demonstrates the mean percent of positive pATM and γH2AX cells of CD3 T cells obtained from each operator before, immediately after, 4 h after, and 24 h after the procedures (Supplement Table S2). Operators A and C show an increase pATM and γH2AX positive cells immediately after the procedures, which moderately decreases 4 h after and further decreases 24 h following the procedures. Operator B shows moderate increase in pATM and γH2AX expression immediately after the procedures and a significant increase 4 h following the procedures. The expression of pATM and γH2AX reduces 24 h following the procedures in all operators. Nevertheless, 24 h after the procedures, operators B and C exhibit pATM and γH2AX expression levels that are above the baseline, whereas operator A shows baseline pATM expression and low, yet above-baseline, levels of γH2AX expression.

The inherent variability of pATM and γH2AX expression between operators was evaluated (Fig. 6). Samples obtained from the four operators were irradiated in vitro at 50.5 μSv (fluoroscopy time 1822 s during 2:15 h procedure) simultaneously. The DAP was 0.0059 Gy*m^2, and the radiation normalized by DAP (radiation DAP) was 8,538 μSv/Gy*m^2. High variability of pATM and γH2AX expression between operators was observed ($p < 0.0001$). The fraction of cells expressing pATM was increased significantly from 0.5 ± 0.1%, 1.8 ± 0.1% and 2.3 ± 0.4% to 18.9 ± 2.0%, 12.5 ± 2.1% and 12.8 ± 1.8% in operators A, C and D, respectively (Fig. 6). Operator B did not demonstrate increase in pATM following irradiation (0.3 ± 0.1% and 0.4 ± 0.2%, without and with irradiation, respectively). The fraction of cells expressing γH2AX increased significantly from 1.9 ± 0.1% and

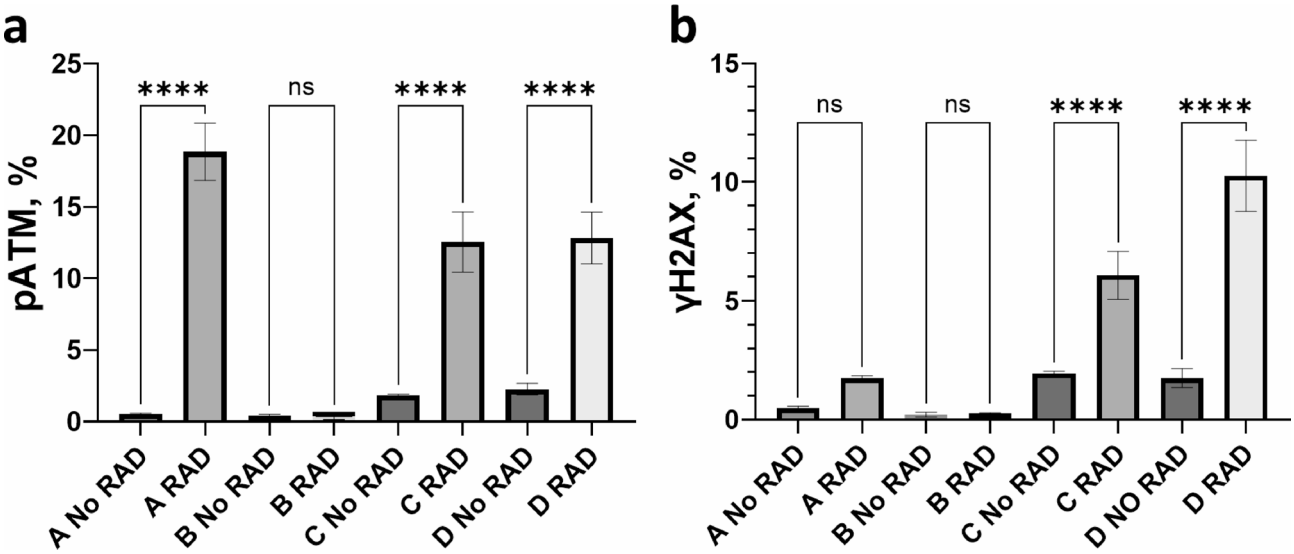

Fig. 6. Variation in the percentage of pATM- and γH2AX-positive lymphocytes following in-vitro irradiation. Two peripheral blood samples (3 ml each) were collected from four operators (A to D). One tube of each operator was irradiated in vitro at 50.5 μSv (fluoroscopy time 1822 s during 2:15 h procedure) simultaneously (RAD), and one tube of each operator was placed at room temperature without radiation during that time (No RAD). The cells were fixed and permeabilized immediately following irradiation and stained with anti-pATM and γH2AX antibodies. The percentage of pATM- and γH2AX-positive lymphocytes was analyzed by flow cytometry. **(A)** Percentage of pATM-positive lymphocytes following incubation, irradiated (RAD) or not irradiated (No RAD). **(B)** Percentage of γH2AX-positive lymphocytes following incubation, irradiated (RAD) or not irradiated (No RAD). ****$p \leq 0.0001$, ns $p > 0.05$. The mean and standard deviations are indicated.

1.8 ± 0.4% to 6.1 ± 1.0% and 10.3 ± 1.5% in operators C and D, respectively ($p < 0.0001$). Operator A demonstrated a trend towards an increase from 0.5 ± 0.1% to 1.8 ± 0.2% ($p = 0.3095$). Operator B did not demonstrate an increase in γH2AX following irradiation (0.2 ± 0.1% and 0.3 ± 0.02%, without and with irradiation, respectively).

Discussion

Fluoroscopically guided EP-interventions expose operators to low-dose X-ray. X-rays can induce DNA damage, such as base damage, oxidation damage, apurinic/apyrimidinic (AP) sites, DNA single-strand breaks, and double-strand breaks (DSB)[13-17]. DSBs are considered the most deleterious lesion, threating the stability of the genome and resulting in mutations, loss of genomic information, chromosomal rearrangements, and cell death. Non-homologous end joining (NHEJ) and homologous recombination are the two main repair mechanisms for DSB repair[28]. Alternative error-prone DSB repair pathways include alternative end joining (alt-EJ) and single-strand annealing (SSA), which contribute to genome rearrangement and oncogenic transformation. Alt-EJ and SSA take over under various conditions depending on the radiation dose, cell cycle phase, and local chromatin environment[28-30]. El-Sayed et al. (2017) demonstrated an acute DNA damage response immediately following fluoroscopically guided endovascular aortic repair interventions, and Abdelhalim et al. (2022) showed a higher incidence of chromosomal aberrations in operators performing a large volume of endovascular procedures[24,25].

The RSS device for fluoroscopic-guided procedures was tested recently during arrhythmia ablation and CIED procedures, demonstrating a significant reduction in the operator's exposure to radiation[26,27]. In the current study, there was an 85% (55-89%) reduction in radiation dose normalized by DAP with RSS. We aimed to determine the effect of the reduced radiation on activation of the acute DNA damage response. Our results indicate that without RSS, both pATM and γH2AX levels increased significantly immediately after EP procedures and gradually decreased over the following 24 h, in line with previous publication performed on endovascular aortic repair interventions[24]. These results indicate that the standard radiation shielding equipment in EP-procedures is insufficient, since the head, arms and feet are exposed to radiation that induce the acute DNA damage response. In the current study, we showed that no pATM and γH2AX expression was detected above baseline following fluoroscopically guided electrophysiologic interventions with the use of RSS protection, suggesting that no acute DNA damage response was activated when using this protection system. We suggest that the RSS protection system reduces radiation exposure to levels below the threshold required to induce DSBs and trigger an acute DNA damage response. This hypothesis can be further investigated by expanding the cohort of operators and including additional study sites. The observed decrease in biomarker levels may suggest a corresponding reduction in the risk of developing health effects, including malignancies and cataracts[1-6].

The proportion of pATM- and γH2AX-positive cells measured immediately after EP-procedures showed a linear correlation with the radiation dose, within the range of 0–185 μSv, as measured by the operators' dosimeters placed over the chest lead apron. Below 13.4 μSv, no significant increase of pATM or γH2AX -positive cells above baseline was detected. Radiation doses in the range of 15 to 55.5 μSv resulted in an increase

in the proportion of pATM- and γH2AX-positive cells above baseline levels in half of the samples. The median radiation reading with RSS was 15 μSv, which explains the low expression of pATM and γH2AX. A more detailed study with more participants assayed with immunohistochemistry as well will enable the determination of the cutoff radiation dose that induces an acute DNA damage repair response involved in DSB repair. This data may provide important information for reliable risk estimation and the establishment of effective protection measures. However, lower radiation doses may produce other types of DNA damage, such as oxidation or base damage, which are also associated with cancer risk. Monitoring DNA repair activities involved in these types of DNA damage may help in defining mechanism-based safety radiation limits and risk estimation[21,31,32].

We estimated the interindividual variability in the induction of pATM and γH2AX expression in $CD3^+$ cells immediately, 4 h, and 24 h after the procedures. While operators A and C demonstrated an immediate increase in pATM and γH2AX positive cells following the procedures, operator B showed a delayed response to radiation. Interindividual variability was also observed following the irradiation of operators' blood samples simultaneously in-vitro with the same radiation dose and duration. While operators A, C and D demonstrated variable increase in the proportion of pATM and γH2AX -positive cells, we could not detect an increase in the proportion of pATM and γH2AX positive cells above baseline in operator B. Interindividual variation in DSB repair efficiency has been observed previously in both humans and mouse models[8,20,33]. High variability in baseline 53BP foci was observed in PBMCs from 674 healthy volunteers, and in ex-vivo irradiated PBMCs obtained from 319 healthy volunteers[34]. These results suggest that susceptibility to radiation may vary between individuals. To optimize radiation protection and establish safety radiation limits, the range of interindividual variability should be evaluated.

The kinetics of pATM and γH2AX expression levels following exposure to radiation were evaluated. Both pATM and γH2AX expression levels were significantly increased immediately following exposure to radiation. This rapid response was also observed in lymphocytes exposed ex-vivo to radiation[35,36]. The pATM positive cells level was reduced to baseline within 24-hours following exposure. The reduction in γH2AX positive cells level was delayed compared to pATM; 4 h after exposure, the γH2AX positive cells level remained as high as immediately after exposure and reduced within 24 h following exposure but remained above baseline. The residual unrepaired breaks may result from the production of complex DNA damage containing two or more lesions in close proximity that may contribute significantly to cell killing and mutations[38–42].

This study does not establish a link between the acute DNA damage response observed and an increased cancer risk or other long-term health outcomes; a larger cohort of operators with chromosomal aberration assay and prospective follow-up is needed. The radiation dose threshold that induced an acute DNA damage repair response was not determined due to the small sample size. The procedures were performed at a single center, this study should be performed in more sites in order to test applicability to other settings. Additionally, the effects of low- dose radiation on other DNA repair mechanisms, such as base excision repair, and on DNA damage and mutations, are unknown and should be studied.

We demonstrated that operators engaged in fluoroscopically-guided electrophysiologic procedures may exhibit a detectable acute DNA damage response, indicating the formation of DSBs and suggest that the standard radiation shielding equipment do not protect the head, arms and feet from X-ray radiation. We showed that the implementation of an effective full-body protection system has the potential to mitigate this genotoxic damage.

Materials and methods

Study participants

This study was approved by the Samson Assuta Ashdod University Medical Center ethics committee (0080-22-AAA) following the principles of the Declaration of Helsinki, and written informed consent was obtained from each participant before the collection of blood samples. Blood samples were taken from 4 operators, basic characteristics are presented in Supplement Table S1. Inclusion criteria: performing EP-procedures at Assuta Ashdod Medical Center, extensive experience with EP procedures including in using the RSS. Exclusion criteria: Healthy without significant illness, smoking, alcohol use, no medication use, no significant exposure to sunlight, the annual cumulative radiation exposure does not exceed the permissible annual dose limit, x-ray examination 48 h before the operation, participation in fluoroscopic intervention 24 h before the study intervention.

Procedural details

All electrophysiological procedures were carried out in an EP laboratory at a single center, Assuta Ashdod Medical Center, Israel, equipped with the Toshiba Infinix fixed X-arm imaging system (Model CAS-830B; DSRX-T7444G) between June 2023 and January 2024. The frame rate used in these procedures was 7–15 frames per second. All four operators had to avoid radiation exposure for at least 24 h prior to the baseline blood samples taken for each experiment. Whenever more than one procedure was included ("consecutive procedures") – the waiting period between them was less than 30 min. In all the EP procedures (CIED implantations and ablations), the operators used a 0.5mmPb lead apron, leaded thyroid collars, leaded goggles, and table-mounted leaded drapes. For ablation procedures, a ceiling-mounted clear lead shield was also used. Blood samples were collected from operators before (baseline), immediately after, 4 h after, and 24 h after they performed EP procedures. The baseline samples were collected no more than 10 min before the operation. The immediately post operation samples were collected within 5 min after the procedure, these criteria were consistent across all experiments. All the samples were transferred immediately to research lab located 30 m from the operation room. An additional baseline blood sample was drawn and placed in a tube next to the C-arm as a positive control. Blood samples were taken from operators for 3 procedures ("isolated" or "consecutive"), each performed on 3 different days, when RSS was not installed in the EP laboratory, and then for 3 procedures when RSS was installed. In one of the 4 operators only one experience was fulfilled without RSS and one with RSS.

The shield system

RSS (Radiaction Ltd., Tel-Aviv, Israel) is a novel robotic system described previously[26,27]. Briefly, the RSS is comprised of upper and lower robotic extendable shields assembled on the C-arm around the X-ray tube and image receptor. It is a lead-free system, with tungsten as the radiation-blocking material. The device utilizes sensors and controls to deploy and retract its attenuating segments, accommodating C-arm angulation and table movement. The system has a small control panel mounted on the table rail next to the C-arm's control panel. Before rotating the C-arm, the operator retracts the shields to allow free C-arm motion. Once the C-arm reaches the desired orientation, the shields are quickly deployed by extending the telescopic segments and their flexible edges. During panning movements, the RSS can be operated in Hover Mode, where the segments are partially deployed. During CIED implantations, we used a "modified RSS deployment mode" in which one of the upper segments remained undeployed so that the surgical field was visible and accessible to the operator.

Standard dosimetry and radiation measurements

Electronic dosimeters were used to record cumulative measurements of the dose equivalence of absorbed radiation in micro-Sievert. Highly sensitive sensors were used for radiation dose measurements (Mirion DMC 3000; Mirion Technologies, Inc). The minimum sensitivity of the Mirion DMC 3000 sensor for a clinical environment was 0.01 μSv. Normalized exposures were calculated by dividing total dose (in μSv) to the Dose Area Product ($Gy \times m^2$). For each operator one dosimeter was attached to the operator's chest (above the operator's protective lead apron). An additional dosimeter was placed next to the positive control blood tube in front of the RSS. The Dose-Area Product (DAP) and fluoroscopy time were recorded for all procedures. All radiation measurements were normalized by the DAP retrieved from the fluoroscopy imaging system at the end of each procedure. Total X-ray time (including total fluoroscopic time and total acquisition time) was taken from the fluoroscopy imaging system at the end of each procedure. Procedure time was measured from the moment the patient entered the room until they left.

Flow cytometry

Peripheral blood samples (about 3 ml) were collected from EP operators in Ethylenediaminetetraacetic acid (EDTA) tubes (BD Biosciences) immediately before, immediately after, 4 h after, and 24 h after the procedures. Within 5 min of each procedure red blood cells were lysed using red blood cells lysis solution (Sartorius) for 10 min at room temperature and then centrifuged for 10 min at 300xg. Cells were diluted to 1×10^6 cells/ml and immediately fixed using Inside Fix (Miltenyi Biotec) for 10 min at room temperature, then centrifuged for 5 min at 500xg (4 °C)[24]. The cells were permeabilized on ice for 30 min with ice-cold (-20 °C) Permeabilzation Buffer A (Miltenyi Biotech) and washed twice with cold buffer (phosphate-buffered saline (PBS), pH 7.2, 0.5% bovine serum albumin (BSA), and 2 mM EDTA). The cells were stained for 30 min in the dark with 1:50 diluted fluorescein isothiocyanate (FITC)-conjugated mouse anti-human CD3 antibody (130-113-128, Miltenyi Biotec), 1:160 diluted (0.125 μg) phycoerythrin (PE)-conjugated anti-human ATM Phospho (Ser1981) antibody (651204, BioLegend), and 1:50 diluted allophycocyanin (APC)-conjugated anti-human H2AX pS139 (γH2AX) REAfinity antibody (130-123-256, Miltenyi Biotech). Fluorescence minus one sample and PE and APC-conjugated IgG isotype controls (BioLegend and Miltenyi Biotech, respectively) were used for gating of pATM and γH2AX. Flow cytometry of 50,000 cells was performed with DxFLEX (Beckman Coulter) flow cytometer and analyzed using CytExpert for DxFLEX software (Beckman Coulter).

Irradiation of blood samples in-vitro.

As an assay positive control, we measured the expression of pATM and γH2AX in blood samples irradiated in-vitro. Before each procedure, 3 ml peripheral blood was collected from each operator in Ethylenediaminetetraacetic acid tubes (BD Biosciences) and positioned about 25 cm from the x-ray source during the procedure and attached to a dosimeter. Immediately after the procedure the tubes were treated as described above for analyzing pATM and γH2AX expression together with the tubes obtained from each operator immediately after the procedure. In order to evaluate the variability between operators in-vitro, 3 ml peripheral blood was collected from 4 operators in Ethylenediaminetetraacetic acid tubes (BD Biosciences) and positioned and treated as described above.

Statistical analysis

GraphPad Prism 10.2.3 (403) (Graphpad Software Inc) and SPSS- version 21 statistical software (IBM.Chicago, Illinois) were used for data analyses. Where appropriate, nonparametric Wilcoxon signed rank, Man-Whitney U and 1-way analysis of variance tests (ANOVA) were used. Multiple comparisons were performed with Tukey's multiple comparisons test or Dunn's multiple comparison test. A p value < 0.05 was considered to be statistically significant. Power analysis was performed using GraphPad Prism, alpha (two tails) = 0.05, the achieved power is 0.85 (total sample size = 20 10 in each group, mean group1 = 1.578, mean group2 = 6.992, standard deviation group 1 = 1.536, standard deviation group 2 = 5.135).

Procedural abbreviations: PVI Cryo = pulmonary vein isolation with cryoballoon anlation catheter; PVI Helius Carto = pulmonary vein isolation with Helius radiofrequency balloon ablation with Carto electroanatomical mapping, Biosense Webster; ICD = implantable cardioverter defibrillator; PPM = permanent pacemaker; EPS = electrophysiological study; CRTD = cardiac resynchronization therapy with defibrillator; CTI-cavo-tricuspid isthmus line. LAO = Left Anterior Oblique, AP = Anteroposterior.

Data availability

The datasets generated during and/or analyzed during the current study are available from the corresponding author on reasonable request.

Received: 6 February 2025; Accepted: 21 May 2025
Published online: 28 May 2025

References

1. Sarkozy, A. et al. Occupational radiation exposure in the electrophysiology laboratory with a focus on personnel with reproductive potential and during pregnancy: A European Heart Rhythm Association (EHRA) consensus document endorsed by the Heart Rhythm Society (HRS). *Europace*. 19 1909–1922 (2017).
2. Yoshinaga, S. et al. Nonmelanoma skin cancer in relation to ionizing radiation exposure among U.S. Radiologic technologists. *Int. J. Cancer*. **115**, 828–834 (2005).
3. Venneri, L. et al. Cancer risk from professional exposure in staff working in cardiac catheterization laboratory: insights from the National research Council's biological effects of ionizing radiation VII report. *Am. Heart J.* **157**, 118–124 (2009).
4. Vano, E., Kleiman, N. J., Duran, A., Romano-Miller, M. & Rehani, M. M. Radiation-associated lens opacities in catheterization personnel: results of a survey and direct assessments. *J. Vasc Interv Radiol.* **24**, 197–204 (2013).
5. Jacob, S. et al. Interventional cardiologists and risk of radiation-induced cataract: results of a French multicenter observational study. *Int J. Cardiol* **167**, 1843–1847 (2013).
6. Roguin, A., Goldstein, J., Bar, O. & Goldstein, J. A. Brain and neck tumors among physicians performing interventional procedures. *Am. J. Cardiol.* **111**, 1368–1372 (2013).
7. Rajaraman, P. et al. Cancer risks in US radiologic technologists working with fluoroscopically guided interventional procedures, 1994–2008. *Am. J. Roentgenol.* **206**, 1101–1108 (2016).
8. Averbeck, D. et al. Establishing mechanisms affecting the individual response to ionizing radiation. *Int. J. Radiat. Biol.* **96**, 297–323 (2020).
9. Kochanova, D. et al. Effects of low-dose ionizing radiation on genomic instability in interventional radiology workers. *Sci. Rep.* **13**, 15525. https://doi.org/10.1038/s41598-023-42139-5 (2023).
10. de Berrington, A. Epidemiological Studies of Low-Dose Ionizing Radiation and Cancer: Rationale and Framework for the Monograph and Overview of Eligible Studies. *J Natl Cancer Inst Monogr*. 97–113 (2020). (2020).
11. UNSCEAR 2015 Sources, Effects and Risks of Ionizing Radiation. UNSCEAR 2012 Report To the General Assembly, with Scientific Annexes. Annex A: Attributing Health Effects To Ionizing Radiation Exposure and Inferring Risks (New York: United Nations Scientific Committee on the Effects of Atomic Radiation) (2015).
12. Hall, J. et al. Ionizing radiation biomarkers in epidemiological studies - An update. *Mutat. Res. Rev. Mutat. Res.* **771**, 59–84 (2017).
13. Laurier, D., Billarand, Y., Klokov, D. & Leuraud, K. The scientific basis for the use of the linear no-threshold (LNT) model at low doses and dose rates in radiological protection. *J. Radiol. Prot.* **43**, 2. https://doi.org/10.1088/1361-6498/acdfd7 (2023).
14. Jackson, S. P. & Bartek, J. The DNA-damage response in human biology and disease. *Nature* **461**, 1071–1078 (2009).
15. Chang, H. H. Y., Pannunzio, N. R., Adachi, N. & Lieber, M. R. Non-homologous DNA end joining and alternative pathways to double-strand break repair. *Nat. Rev. Mol. Cell. Biol.* **18**, 495–506 (2017).
16. Zhao, B., Rothenberg, E., Ramsden, D. A. & Lieber, M. R. The molecular basis and disease relevance of non-homologous DNA end joining. *Nat. Rev. Mol. Cell. Biol.* **21**, 765–781 (2020).
17. Shiloh, Y. ATM and related protein kinases: safeguarding genome integrity. *Nat. Rev. Cancer*. **3**, 155–168 (2003).
18. Weiss, C. N., Ito, K. D. N. A. & Damage A sensible mediator of the differentiation decision in hematopoietic stem cells and in leukemia. *Int. J. Mol. Sci.* **16**, 6183–6201 (2015).
19. Valente, D. et al. Factors to consider for the correct use of γH2AX in the evaluation of DNA Double-Strand breaks damage caused by ionizing radiation. *Cancers (Basel)*. **14**, 6204. https://doi.org/10.3390/cancers14246204 (2022).
20. Penninckx, S., Pariset, E., Cekanaviciute, E. & Costes, S. V. Quantification of radiation-induced DNA double strand break repair foci to evaluate and predict biological responses to ionizing radiation. *NAR Cancer*. **3**, zcab046. https://doi.org/10.1093/narcan/zcab046 (2021).
21. Sevilya, Z. et al. Low integrated DNA repair score and lung cancer risk. *Cancer Prev. Res. (Phila)*. **7**, 398–406 (2014).
22. Maffei, F. et al. Spectrum of chromosomal aberrations in peripheral lymphocytes of hospital workers occupationally exposed to low doses of ionizing radiation. *Mutat. Res.* **547**, 91–99 (2004).
23. Lee, W. H., Nguyen, P. K., Fleischmann, D. & Wu, J. C. DNA damage-associated biomarkers in studying individual sensitivity to low-dose radiation from cardiovascular imaging. *Eur. Heart J.* **37**, 3075–3080 (2016).
24. El-Sayed, T. et al. Radiation-Induced DNA damage in operators performing endovascular aortic repair. *Circulation* **136**, 2406–2416 (2017).
25. Abdelhalim, M. A. et al. Higher incidence of chromosomal aberrations in operators performing a large volume of endovascular procedures. *Circulation* **145**, 1808–1810 (2022).
26. Laish-Farkash, A. et al. A novel robotic radiation shielding device for interventional cardiology procedures. *EuroIntervention* **18**, 262–266 (2022).
27. Laish-Farkash, A. et al. A novel robotic radiation shielding device for electrophysiologic procedures: A prospective study. *Am. Heart J.* **261**, 127–136 (2023).
28. Scully, R., Panday, A., Elango, R. & Willis, N. A. DNA double-strand break repair-pathway choice in somatic mammalian cells. *Nat. Rev. Mol. Cell. Biol.* **20**, 698–714 (2019).
29. van de Kooij, B., Kruswick, A., van Attikum, H. & Yaffe, M. B. Multi-pathway DNA-repair reporters reveal competition between end-joining, single-strand annealing and homologous recombination at Cas9-induced DNA double-strand breaks. *Nat. Commun.* **13**, 5295. https://doi.org/10.1038/s41467-022-32743-w (2022).
30. Mladenov, E., Mladenova, V., Stuschke, M. & Iliakis, G. New facets of DNA double strand break repair: radiation dose as key determinant of HR versus c-NHEJ engagement. *Int. J. Mol. Sci.* **24** (14956). https://doi.org/10.3390/ijms241914956 (2023).
31. Paz-Elizur, T. et al. DNA repair biomarker for lung Cancer risk and its correlation with airway cells gene expression. *JNCI Cancer Spectr.* **4**, pkz067. https://doi.org/10.1093/jncics/pkz067 (2019).
32. Sevilya, Z. et al. Development of APE1 enzymatic DNA repair assays: low APE1 activity is associated with increase lung cancer risk. *Carcinogenesis* **36**, 982–991 (2015).
33. Wilson, P. F. et al. Inter-individual variation in DNA double-strand break repair in human fibroblasts before and after exposure to low doses of ionizing radiation. *Mutat. Res.* **683**, 91–97 (2010).
34. Pariset, E. et al. DNA damage baseline predicts resilience to space radiation and radiotherapy. *Cell. Rep.* **33** (108434). https://doi.org/10.1016/j.celrep.2020.108434 (2020).
35. Sharma, P. M. et al. High throughput measurement of γH2AX DSB repair kinetics in a healthy human population. *PLoS One*.10, e0121083;10.1371/journal.pone.0121083 (2015).
36. Lee, Y., Wang, Q., Shuryak, I., Brenner, D. J. & Turner, H. C. Development of a high-throughput γ-H2AX assay based on imaging flow cytometry. *Radiat. Oncol.* **14** (150). https://doi.org/10.1186/s13014-019-1344-7 (2019).
37. Tsao, D. et al. Induction and processing of oxidative clustered DNA lesions in 56Fe-ion-irradiated human monocytes. *Radiat. Res.* **168**, 87–97 (2007).
38. Lopez Perez, R. et al. DNA damage response of clinical carbon ion versus photon radiation in human glioblastoma cells. *Radiother Oncol.* **133**, 77–86 (2019).

39. Wilkinson, B., Hill, M. A. & Parsons, J. L. The cellular response to complex DNA damage induced by ionising radiation. *Int. J. Mol. Sci.* **24**, 4920. https://doi.org/10.3390/ijms24054920 (2023).
40. Bhogal, N. et al. Late residual gamma-H2AX foci in murine skin are dose responsive and predict radiosensitivity in vivo. *Radiat. Res.* **173**, 1–9 (2010).
41. Nikjoo, H. et al. Modelling of DNA damage induced by energetic electrons (100 eV to 100 keV). *Radiat. Prot. Dosimetry*. **99**, 77–80 (2002).
42. Goodhead, D. T. Energy deposition stochastics and track structure: what about the target? *Radiat. Prot. Dosimetry*. **122**, 3–15 (2006).

Author contributions

Conceptualization, ZS, ALF and EL; methodology, ZS.; validation, EL, EB; investigation, ZS, MR, YK, GM, MC, VH, ALF; writing—original draft preparation, ZS; writing-review and editing, ZS, MR, YK, GM, MC, VH, and ALF; visualization, ZS; supervision, ALF; project administration, ZS and ALF; funding acquisition, ALF; All authors have read and agreed to the published version of the manuscript.

Funding

This study was supported by an unrestricted grant from Assuta Ashdod Medical Center and by Radiaction Ltd., which contributed funding specifically for the reagents utilized in this project. The funding bodies had no role in the study design, data collection, analysis, or decision to publish the manuscript.

Competing interests

This work was supported by an unrestricted grant from Assuta Ashdod Medical Center and from Radiaction Ltd. The funding bodies had no role in the study design, data collection, analysis, or decision to publish the manuscript. All authors of this manuscript have no competing interest.

Additional information

Supplementary Information The online version contains supplementary material available at https://doi.org/10.1038/s41598-025-03686-1.

Correspondence and requests for materials should be addressed to Z.S.